Quantum Electronics **47** (12) 1158–1165 (2017)

INTERACTION OF LASER RADIATION WITH MATTER. LASER PLASMA https://doi.org/10.1070/QEL16512

Laser-induced transfer of gel microdroplets for cell printing

V.I. Yusupov, V.S. Zhigar'kov, E.S. Churbanova, E.A. Chutko, S.A. Evlashin, M.V. Gorlenko, V.S. Cheptsov, N.V. Minaev, V.N. Bagratashvili

Abstract. **We study thermal and transport processes involved in the transfer of gel microdroplets under the conditions of laser cell microprinting. The specific features of the interaction of pulsed laser radiation (λ = 1.064 μm, pulse duration 4–200 ns, energy 2 μJ–1 mJ) with the absorbing gold film deposited on the glass donor substrate are determined. The investigation of the dynamics of transport processes by means of fast optical video recording and optoacoustic methods makes it possible to determine the characteristics of the produced gel jets as functions of the laser operation regimes. The hydrodynamic process of interaction between the laser radiation and the gold coating with the hydrogel layer on it is considered and the temperature in the region of the laser pulse action is estimated. It is shown that in the mechanism of laser-induced transfer a significant role is played by the processes of explosive boiling of water (in gel) and gold. The amount of gold nanoparticles arriving at the acceptor plate in the process of the laser transfer is determined. For the laser pulse duration 8 ns and small energies (less than 10 μJ), the fraction of gold nanoparticles in the gel microdroplets is negligibly small, and their quantity linearly grows with increasing pulse energy. The performed studies offer a base for optimising the processes of laser transfer of gel microdroplets in the rapidly developing technologies of cell microprinting.**

Keywords: *laser-induced transfer, gel microdroplets, cell printing.*

1. Introduction

The technologies of laser-induced forward transfer of matter [1–6] are widely used in biomedicine for printing biological materials [7–9], for printing stem cells in the cell engineering [10], for printing functioning organs [11], for deposition of DNA or protein on biochips [12], for isolating individual cells [13], and, lately, for microsampling of microorganisms which are hard to cultivate [14].

For implementing the laser-induced transfer, a layer of substrate (usually gel with cells) is deposited on the donor plate, consisting of a glass plate with a thin absorbing (usually metallic) coating on the working side. The radiation of a pulsed laser is focused on the absorbing layer. Under the effect of the short laser pulse, a small part of the absorbing layer is evaporated, giving rise of a pressure jump that causes the transfer of a gel substrate microdroplet to the acceptor plate. The characteristics of the laser transfer process depend on the parameters of the laser pulse (wavelength, duration, energy, intensity and focusing parameters), the composition, thickness and structure of the absorbing coating, as well as on the thickness of the gel substrate layer, its composition, homogeneity, viscosity, surface tension value, the material of donor and acceptor plates. It is important that the technology of the laser transfer allows purposeful transfer of the required microscopic quantity of substance (individual cells or their agglomerates, particles of biotissues and carriers of cells and microorganisms).

In the transfer of living systems, the success of technology is determined by the possibility to provide the transfer of the needed amount of cell-gel substrate from the donor plate to the acceptor one without destructing the cell system structure. A number of physical factors can affect the cell systems, transferred by means of laser printing: (i) the pulsed laser radiation, transmitted through the absorbing film; (ii) the shock waves; (iii) the high temperatures; (iv) the broadband optical radiation, related to the fast laser heating of the material of the absorbing film and plasma formation; and (v) the nanoparticles of the absorbing film that can be transferred to the acceptor substrate together with the gel. Therefore, the determination of the effect of such processes on the cells and its minimisation is an urgent problem.

In the present paper, we consider thermal and transport processes that occur in the course of transferring microscopic volumes of the gel-based substrate (2% aqueous solution of hyaluronic acid) under the impact of nanosecond pulses of laser radiation with the wavelength 1.064 μm. The energy of the laser pulses passed through the gold absorbing film is measured. The content of gold nanoparticles in a microdroplet on the acceptor substrate as a function of the laser pulse energy is determined.

2. Material and methods

To implement the laser transfer we used the radiation of a YLPM-1-4x200-20-20 pulsed fibre laser (NTO 'IRE-Polus', Russia) having the wavelength 1064 nm, the pulse duration 4–200 ns, the pulse energy 2 μJ–1 mJ and the close-to-Gaussian beam intensity profile ($M^2 < 1.5$). The scanning of the laser radiation was implemented by means of an LscanH-10-1064 two-mirror Galvano scanning head (AtekoTM, Russia) with

V.I. Yusupov, V.S. Zhigar'kov, E.S. Churbanova, E.A. Chutko, N.V. Minaev, V.N. Bagratashvili Institute of Photonic Technologies, Federal Research Centre 'Crystallography and Photonics', Russian Academy of Sciences, ul. Pionerskaya 2, Troitsk, 108840 Moscow, Russia; e-mail: iouss@yandex.ru;
S.A. Evlashin Skolkovo Institute of Science and Technology, Centre for Design, Manufacturing and Materials, ul. Novaya 100, Skolkovo, 143025 Moscow, Russia;
M.V. Gorlenko, V.S. Cheptsov M.V. Lomonosov Moscow State University, Vorob'evy Gory, 119991 Moscow, Russia

Received 1 September 2017
Kvantovaya Elektronika **47** (12) 1158–1165 (2017)
Translated by V.L. Derbov

an SL-1064-110-160 F-theta objective (Ronar-Smith, Singapore), having the focal length 160 mm that allows the laser radiation to be focused on the irradiated surface into a spot 30 μm in diameter.

As donor plates we used AG00000112E standard rectangular glass slides (Menzel, Thermo Fisher Scientific), on which a layer of gold 50 nm thick was deposited using the magnetron sputtering method [15]. The film thickness was determined using a LOMO MII4 optical profilometer. The donor plate was fixed on a magnetic holder with the gold coating facing downward, so that the coating was located in the objective focal plane with the accuracy no worse than 100 μm.

As a substrate in the laser transfer experiments, we used the gel based on the hyaluronic acid (2% aqueous solution). The gel viscosity determined with a Micro VISC viscosimeter (RheoSense, USA) amounted to 15.5 ± 0.05 mPa s. In some of the experiments aimed at the study of transport processes in laser microsampling of microorganism carriers, the particles of soil having the size smaller than 300 μm (200 mg of soil per 1.4 mL of gel) were added to the gel. In the process of preparing the donor plate to the experiments, a layer of working fluid (pure gel or gel with soil) having the thickness 200 ± 30 μm was applied to the gold layer. To this end, the donor plate was placed horizontally on a motorised translation stage, and a drop (100 μL) of working fluid was applied to it and spread uniformly with the edge of a knife, installed with the necessary gap above the surface.

Figure 1 presents a schematic of the setup for laser-induced transfer of the substrate. The radiation from the pulsed laser, passed through the beam shaper and the scanner, was focused on the absorbing coating of the donor plate. The microdroplets of substrate obtained under laser irradiation were collected on the acceptor plate, installed at the distance 1 mm from the bottom surface of the donor plate.

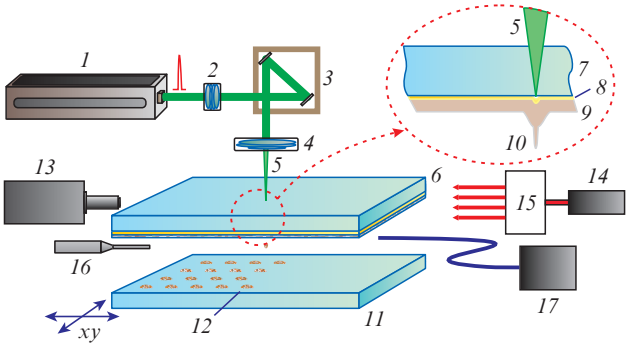

Figure 1. Schematic of the setup for laser-induced transfer of gel microdroplets:
(*1*) pulsed laser; (*2*) beam shaper; (*3*) scanner; (*4*) objective; (*5*) focused beam; (*6*) donor plate; (*7*) glass plate; (*8*) Au layer; (*9*) substrate layer; (*10*) substrate jet; (*11*) acceptor plate; (*12*) microdroplets; (*13*) fast video camera; (*14*) continuous-wave laser; (*15*) telescope; (*16*) needle hydrophone; (*17*) fibre spectrometer.

The optical recording of the laser-induced transport processes was carried out using a Fastcam SA-3 video camera (Photron, Japan) at a rate up to 60000 frames per second. The illumination was implemented using the radiation of a cw laser diode (*14*) with the wavelength 660 nm, shaped by a telescope (*15*) to get a circular beam with the diameter 14 mm. To control the spectral composition and the power of the accompanying optical radiation, we used a USB4000 optical fibre spectrum analyser (Ocean Optics, USA) with the resolution ~1.5 nm (the spectral range 200–1100 nm), connected to a personal computer.

To control the dynamics of laser-induced processes, besides the optical method, we also used the optoacoustic one [16, 17]. The acoustic signals were detected by a needle hydrophone (Precision Acoustics, Great Britain) having the diameter 1 mm with a preamplifier with the band 10 kHz–50 MHz (the sensitivity –241 dB relative to 1 V Pa^{-1}) and recorded using a DS 72304 four-channel digital memory oscilloscope (GW Instek, Taiwan) with the transmission band 300 MHz. During the experiment, the working part of the hydrophone was placed in a microcuvette with water, the surface of which touched the absorbing layer of the plate. Thus, an acoustic contact between the region of the absorbing layer affected by the laser pulse and the sensitive element of the hydrophone was provided. The distance from the face of the hydrophone to the laser beam focusing spot on the film amounted to ~4 mm. The optoacoustic method was also used to estimate the absorption coefficient K_f of the pulsed laser radiation in the gold film. To this end, the amplitudes of the acoustic pulses from the gold film (P_1) were compared with the amplitude of pulses obtained by laser irradiation of the substrates with carbon film (P_2). The carbon layer thickness amounted to ~1 μm and was sufficient for complete absorption of the laser radiation with the wavelength 1064 nm. Since the amplitude of the acoustic pulse is proportional to the absorbed energy of laser radiation [18, 19], the value of K_f was estimated from the relation $K_f = P_1/P_2$.

The optical properties of the films were measured in the range 200–800 nm using a Cary 50 Scan spectrometer (Agilent, USA), and in the range 700–2000 nm with a UV-360 spectrometer (Shimadzu, Japan). The energy of the pulsed laser radiation was controlled using a S310C thermosensor for power measurement (Thorlabs, USA) and a S144C photodiode detector for power measurement in combination with a PM100D digital measurement control panel (all Thorlabs devices, USA). The samples were studied using an HRM-300 Series optical 3D microscope (Huvitz, Korea) and a PHENOM ProX scanning electron microscope (SEM) (Phenom World, the Netherlands) with the energy-dispersive detector unit.

The presence of gold in the gel droplets at the acceptor plate was determined from the SEM images using the data of the energy-dispersive analysis. Using this analysis, the gold nanoparticles were selected in the SEM grey-scale image and their brightness B_i was estimated; the mean value $\bar{B}_i$ and the standard deviation Δ were determined. Then the SEM image was processed using the MATLAB software package. Compact areas of the image with $B_i \geqslant \bar{B}_i - \Delta$ were attributed to gold nanoparticles.

3. Results

Figure 2 presents the spectrum of low-intensity optical radiation transmission through the donor plate with the gold film. With increasing wavelength the transmission coefficient T_{tr} grows, achieves a maximum at $\lambda \approx 500$ nm and then monotonically decreases. At the operating wavelength of the laser (1064 nm), ~0.15% of optical energy is transmitted through the gold layer.

The impact of short high-power laser pulses leads to the formation of holes in the gold film on the donor plate. The holes are clearly distinguishable by means of the optical microscope (Fig. 3). The holes in the film have nearly circular

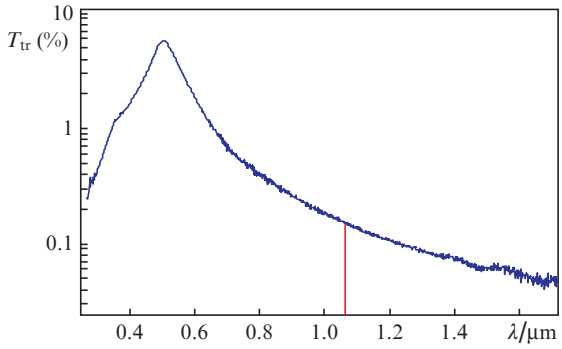

Figure 2. Spectrum of transmission of low-intensity optical radiation through the donor plate with the 50-nm-thick gold film. The laser radiation wavelength is marked.

shape and contain relatively dark areas inside having the shape of concentric circles of rings. With increasing laser pulse energy E (in μJ), the hole diameter (in μm) increases nearly as $19E^{0.26}$, and the outer diameter of the inner dark areas as $12E^{0.33}$.

When the donor plate is covered with a layer of substrate, the parameters of laser-produced holes in the gold film and their inner structures change. Figure 4 presents the SEM images of a hole in the gold film obtained at different energies of laser pulses without using gel and with the gel applied to the donor plate. It is seen that the application of gel essentially changed the structure of the holes: (i) their size has changed; (ii) a thick edging of film fragments bent outside the hole has appeared; and (iii) the diameter of inner areas has sharply decreased.

Figure 5 presents the SEM images of a fragment of the donor plate after pulsed irradiation (τ = 8 ns, E = 20 μJ) and fragments of the ring in the inner part of the hole in different scales. From Fig. 5b one can see that the ring in the inner part of the hole consists of gold nanoparticles, the size of which monotonically grows on average from 30–50 nm near the centre to 100–200 nm at the periphery.

Under the action of a high-power laser pulse on the donor plate, one can observe a bright flash of light. Figure 6 presents individual frames of the fast video record, obtained using the Fasctcam SA-3camera, in which the glowing regions are observed at different laser pulse energies. It is seen that with increasing pulse energy, the size of these regions increases and their transverse size essentially exceeds the width of the laser beam spot at the absorbing film. Note that at E = 0.2 mJ the glowing region is located in the glass above the Au film. With increasing energy a glowing region also appears in the air. The spectral characteristics of this optical radiation (a broadband radiation with characteristic narrow lines) allow the conclusion that it is emitted by plasma.

When the laser pulses act on the donor substrate with the gel layer, thin jets of gel are formed (Fig. 7) in the case of the pulse energy exceeding the threshold energy ($E_{th} \approx 0.05$ mJ). When the energy of the laser pulse is below the threshold, a hardly seen swelling is observed in the region of the laser

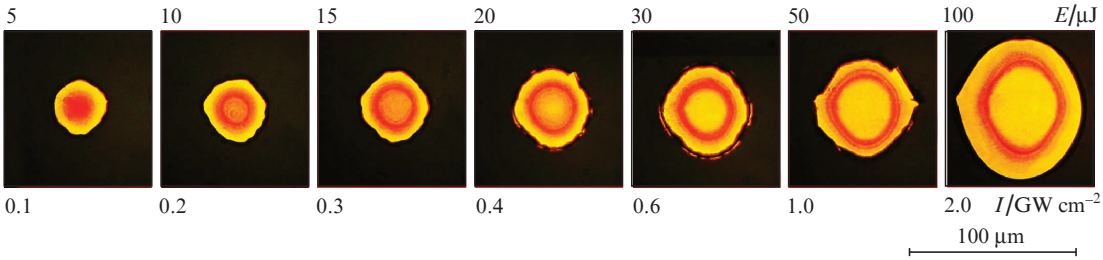

Figure 3. Transmitted-light optical images of the holes in the gold film produced by the laser pulses having different energy E and radiation intensity I; τ = 8 ns.

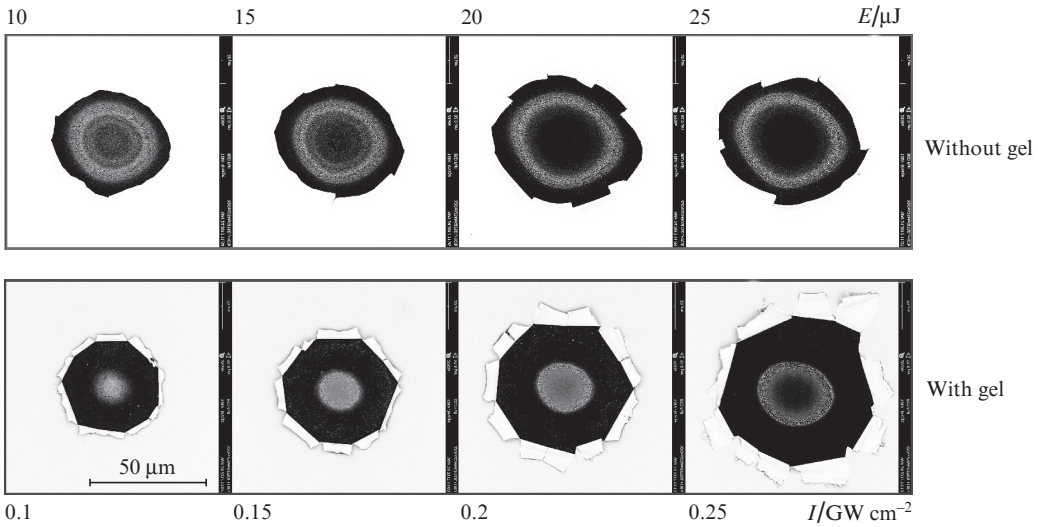

Figure 4. SEM images of the holes in the gold film obtained at different energies of the laser pulses and radiation intensities without gel and in the presence of gel on the donor plate; τ = 8 ns.

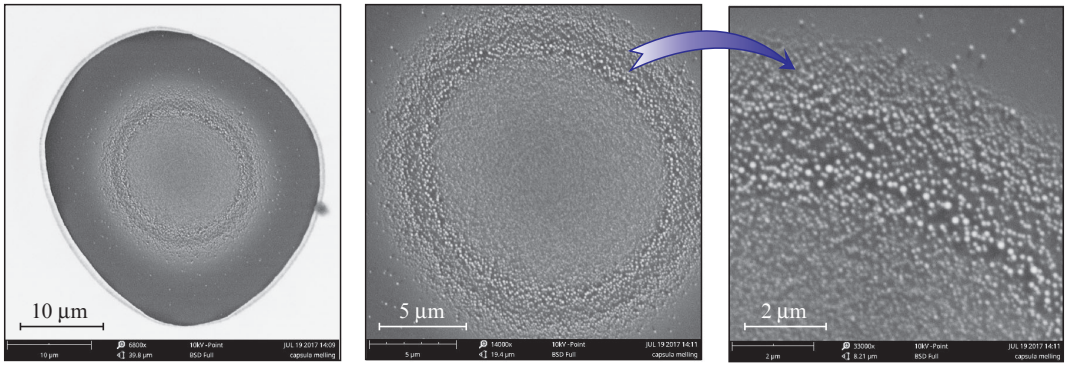

Figure 5. (a) SEM image of a fragment of the donor plate with a gold film after pulsed laser irradiation (τ = 8 ns, E = 20 μJ, I = 0.4 GW cm^{-2}) and (b, c) magnified fragments of the ring consisting of gold nanoparticles.

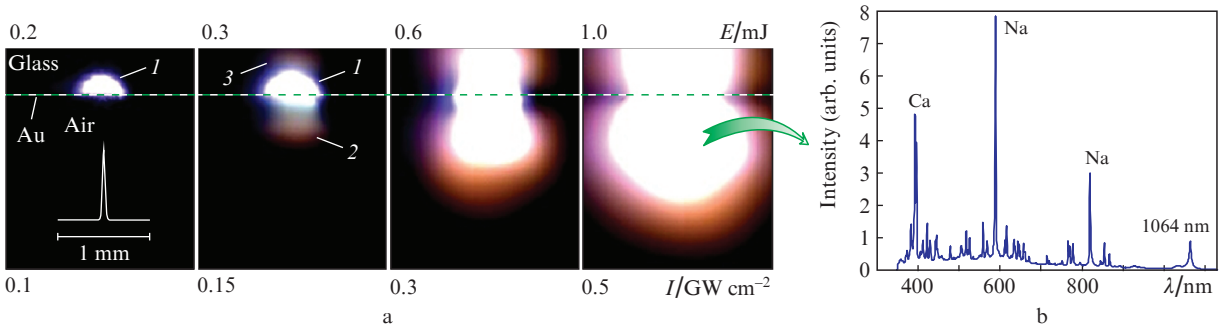

Figure 6. (a) Frames of the video record of optical radiation under the impact of laser pulses having different energies E and intensities I at the donor plate [(*1*) heated glass region, (*2*) plasma, (*3*) reflection of the glowing plasma) and (b) spectrum of the optical radiation for E = 1 mJ. In the first frame the radial distribution of the laser radiation intensity is schematically shown for the axial intensity 8.8×10^7 W cm^{-2}. The dashed line shows the gold film position.

impact. With the increase in energy a thin jet of gel appears, the swelling diameter first decreases (at E = 70 μJ) and then monotonically increases. At E = 70 μJ the jet extends beyond the frame boundary and its velocity exceeds 40 m s^{-1}. In the region of large energies ($E \geqslant 0.2$ mJ) the glowing region (*3*) (Fig. 7) arises in the gel near the gold film.

The dependences of the coefficient of transmission of the radiation through the gold film on the laser pulse energy at τ = 8–20 ns are presented in Fig. 8. Practically for all curves with the growth of energy one can observe a gradual decrease in the transmission coefficient T_{tr}. The exceptions are the cases with τ = 4 ns and two first points for the pulse duration 8 and 20 ns, for which T_{tr} increases with increasing energy. The maximal values of the transmission coefficient for small τ amounted to 36.0%±4.2% for τ = 20 ns and E = 17 μJ (Fig. 8a), and for large τ to 60.0%±4.3% for τ = 300 ns and E = 160 μJ (Fig. 8b). The smallest recorded value of T_{tr} for small τ equals 6.1%±2.4% for τ = 4 ns, E = 24 μJ, Φ = 1 J cm^{-2} (Fig. 8a) and for large τ 10.3%±2.5% for τ = 30 ns, E = 235 μJ, Φ = 75 J cm^{-2} (Fig. 8b). Here Φ is the laser pulse energy density.

The acoustic signals recorded under the impact of the laser pulse on the donor plates with a gold layer and a carbon layer

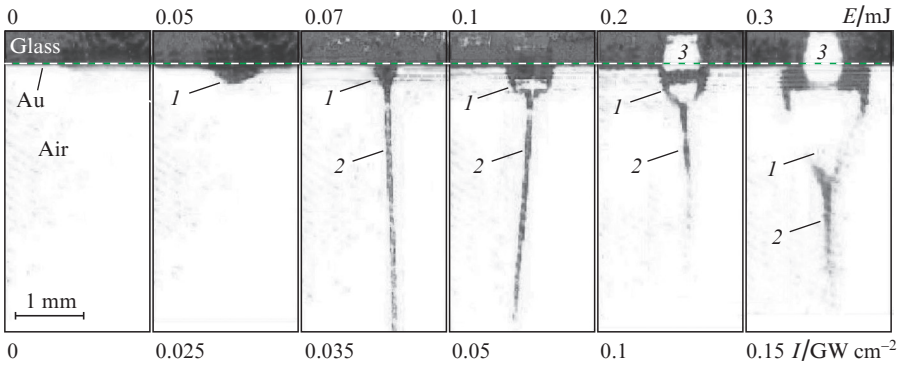

Figure 7. Formation of gel jets under the action of laser pulses with different energies and intensities (τ = 200 ns) on the donor plate: (*1*) bubble, (*2*) gel jet; (*3*) glowing plasma. The dashed line shows the gold film position. The recording rate is 10000 frames per second.

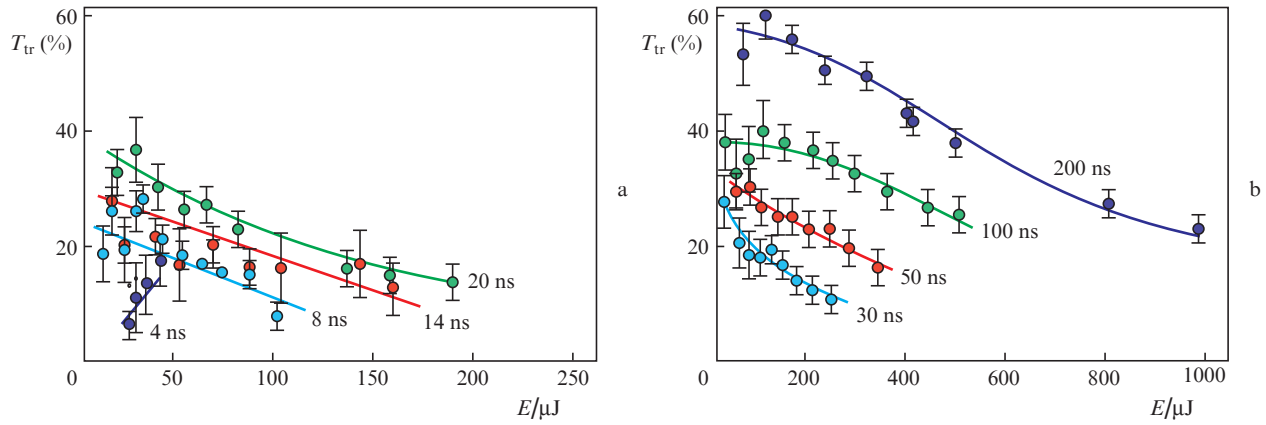

Figure 8. Dependences of the coefficient of transmission of laser radiation through the gold film on the pulse energy for (a) small and (b) large durations of the pulse (indicated at the curves).

are presented in Fig. 9. The first acoustic signal reaches the hydrophone in $\tau \approx 1$ μs after the laser impact, and in ~3 μs the high-power acoustic pulses arrive with the amplitudes P_1 and P_2, after which the high-frequency oscillations of pressure are observed with the period, gradually growing from 0.1 to 0.7 μs. The obtained data allow the coefficient of absorption of the pulsed laser radiation in the gold film to be estimated as $K_f = P_1/P_2 \approx 18\% \pm 4\%$.

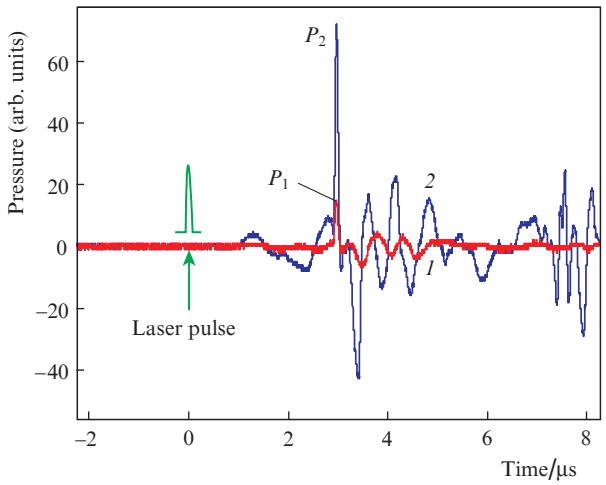

Figure 9. Acoustic signals recorded under the laser pulse action ($\tau = 8$ ns, $E = 20$ μJ, $I = 0.4$ GW cm^{-2}) on the plates with (*1*) a gold layer and (*2*) a carbon layer; P_1 and P_2 are high-power acoustic pulses.

Figure 10 presents the examples illustrating some features of the distribution of gold nanoparticles in the gel droplets on the acceptor substrate. The results of the mathematical processing of SEM images have shown that practically in all cases a certain amount of gold nanoparticles are present in the gel droplets (Fig. 10a). At large energies of laser pulses one can find fragments of the Au film inside the droplet and sometimes outside it on the acceptor plate (Fig. 10b). In some cases, the transferred gold nanoparticles are distributed over the substrate not randomly, but, e.g., as filament structures (Fig. 10c). The experiments have shown that the amount of gold in the gel droplets in the form of nanoparticles and microparticles depends on the laser pulse energy E and duration τ and grows on average with E. Thus, for $\tau = 8$ ns the content of nanoparticles S_{Audr}, equal to the ratio of their area in the SEM images to the droplet area (in %) in a wide range of energies of the laser pulse (5 μJ $\leqslant E \leqslant$ 100 μJ), demonstrates practically linear dependence on E: $S_{Audr} \approx 0.01E$.

The experiments on microsampling of the substrate consisting of gel with microparticles of soil have shown that their addition to the gel essentially changes the parameters of the microdroplet transport. Figure 11 presents examples of fast

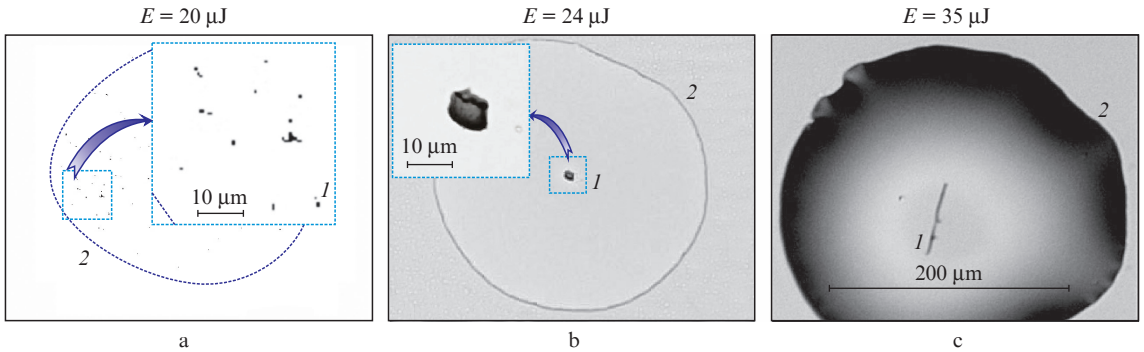

Figure 10. Example distributions of micro- and nanoparticles of gold in the gel droplets at different energies of the laser pulse: (a) the result of mathematical selection of gold nanoparticles in the SEM images of the droplet, (b) SEM image of the droplet with a microparticle of gold, and (c) the filament structure of gold nanoparticles; (*1*) nanoparticles or microparticles of gold; (*2*) gel droplet contour. The insets show magnified images of the droplet fragments.

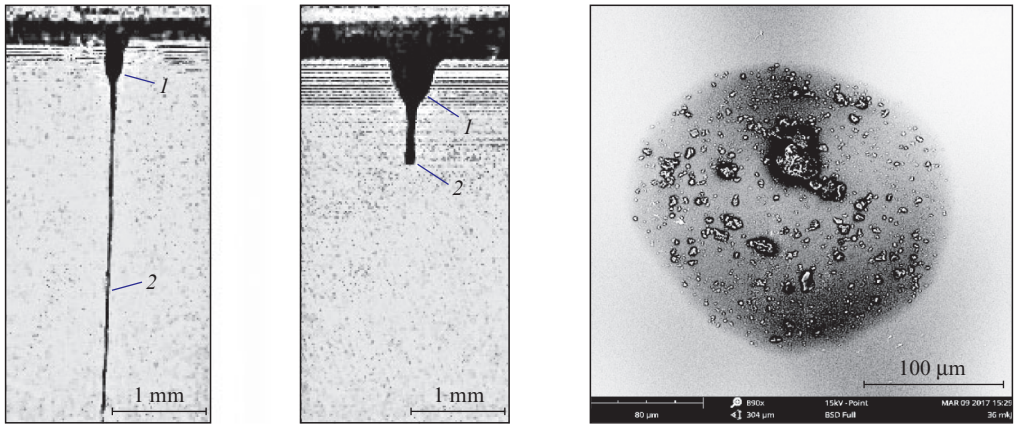

Figure 11. Generation of jets under the impact of the laser pulse (τ = 8 ns, E = 10 μJ) on the donor plate with (a) pure gel and (b) the gel containing microparticles of soil, as well as (c) the SEM image of a gel droplet with the particles of soil: (*1*) bubble; (*2*) jet of substrate gel.

record frames with images of gel jets in two cases, namely, with pure gel (Fig. 11a) and with gel containing soil microparticles (Fig. 11b). It is seen that the addition of particles leads to the thickening of both the jet itself and the bubble at its base (Fig. 11b), and the jet velocity decreases by nearly 6 times. The volumes of the jets in Fig. 11b remained almost unchanged (5 nL in the case of gel and 5 nL in the case of substrate). The transfer of the substrate leads to the formation of the drop having the diameter 224 ± 12 μm on the acceptor plate, inside which over the entire area the soil particles can be seen having the size from 1 to 30 μm (Fig. 11c).

4. Discussion

The experiments have shown that the absorption of short high-power laser pulses in the gold film on the donor plate causes the formation of almost circular holes in the film (Figs 3, 4), containing relatively dark regions having the shape of concentric circles or rings. With increasing laser pulse energy, the size of the holes and the above regions, consisting of gold nanoparticles, monotonically increases. Comparing the size of the holes at different pulse energies and assuming the laser beam to be Gaussian, it is easy to estimate the threshold intensity for hole formation in the film ($I_{\text{th}} \approx 4\times10^7$ W cm^{-2}, which corresponds to the energy density $\Phi_{\text{th}} \approx 0.3$ J cm^{-2}). The absorption of laser radiation causes the fast heating of the film area to high temperatures and the hole formation. In metals the laser radiation is absorbed by electrons and then during the time interval 1–10 ps the energy is transferred to atoms in the process of electron-lattice relaxation [20], which leads to the fast bulk heating of the material. This heating in nanosecond scale gives rise to a recoil pulse related to the fast material expansion, melting and evaporation of part of the Au film, as well as to the formation of a plasma torch [20] (see also Fig. 6).

In the presence of a gel layer on the donor plate, the structure of laser-produced holes in the gold film cardinally changes (Fig. 4). The size of the inner regions of the holes containing nanoparticles of gold essentially decreases, and the thick edging appears that consists of the fragments of gold film deflected from outside. We believe that these effects are related to the formation and cavitation collapse of bubbles [21] arising under pulsed laser heating (Fig. 7). Such a bubble appears due to the explosive boiling of water in the gel [17], and at relatively high temperatures (in the case of large intensities of laser radiation) due to the explosive boiling of gold [22] and plasma formation (see Fig. 6 for $E \geqslant 0.3$ mJ and Fig. 7 for $E \geqslant 0.2$ mJ). After the expansion to the maximal size, the bubble in the gel experiences the cavitation collapse [21]. As a result, the atoms and nanoparticles of gold located in this region near the surface of the substrate and at the surface of the bubble [23] gather in the centre of the laser-induced hole into a structure with the size smaller than in the absence of the gel (Fig. 4). As seen from Fig. 7, the laser-induced hydrodynamic processes considered above lead not only to the formation of a bubble in the gel, but also to the appearance of a thin jet of gel (Fig. 7) moving towards the acceptor substrate (see Fig. 1) with a high velocity exceeding 40 m s^{-1} at I = 35 MW cm^{-2}.

The gold film and the gel area contacting with it are heated as a result of the absorption of laser radiation in the film. For small intensities, the absorption spectrum of thin gold films is studied sufficiently well [24]. In our case, when the heating to high temperatures occurs, leading to an abrupt fall of the laser radiation reflection coefficient [25], melting and evaporation of gold and even plasma formation (Fig. 6), the estimate of the absorption coefficient K_{f} was obtained using the optoacoustic method. For this purpose, we compared the amplitudes of the laser-induced acoustic pulses (P_1 and P_2 in Fig. 9) under the impact of the laser pulse on the substrates with the films of gold and carbon, in the layer of which the laser radiation is completely absorbed. Since the amplitudes of the acoustic pulses are proportional to the absorbed laser energy [18, 19], $K_{\text{f}} = P_1/P_2$. In the optoacoustic experiment, the value of the absorption coefficient of the gold film was determined for the pulsed laser radiation with τ = 8 ns, E = 20 μJ, and I = 0.4 GW cm^{-2} as $K_{\text{f}} \approx 18\% \pm 4\%$.

The gradual heating of the gold film to the temperature $T(t)$ as a result of the laser pulse impact is accompanied with the following processes. Simultaneously with the gold film, the thin layers of glass and gel consisting mainly of water are heated to this temperature. The depth of thermal heating will increase with time t, thus, for the glass $d_T^{\text{g}} = \sqrt{4D_T^{\text{g}}t}$, where $D_T^{\text{g}} = 3.4\times10^{-7}$ m^2 s^{-1} is the thermal diffusivity coefficient of glass, and for the gel (water) $d_T^{\text{w}} = \sqrt{4D_T^{\text{w}}t}$, where $D_T^{\text{w}} = 1.4\times10^{-7}$ m^2 s^{-1} is the thermal diffusivity coefficient of water.

At the temperature $T_1 = (0.9 - 1)T_c^w \approx 600$ K, where $T_c^w = 647.1$ K is the critical temperature of water, in the heated layer of water the explosive boiling of water occurs [26] with the formation of rapidly expanding bubbles in the region of the laser impact. At $T_2 = 1336$ K the gold film starts melting, and at $T_3 \approx 7000$ K ($T_c^{gold} = 7250$ K) its explosive boiling with the formation of expanding bubble begins. Since the critical pressure for gold is very high (~500 MPa) and essentially exceeds the critical pressure for water (~22 MPa), a fraction of particles and atoms of gold reach the wall of the expanding bubble and penetrate into the gel. The kinetic energy absorbed in the gel leads to the acceleration of the gel jet.

The temperature in the region of the laser impact at the end of the laser pulse ($t = \tau$) can be estimated using the expression [27]

$$T = T_0 + \frac{\Phi_{abs}}{\rho^g C_p^g d_T^g + \rho^{gold} C_p^{gold} h + \rho^w C_p^w d_T^w}, \quad (1)$$

where $T_0 \approx 300$ K is the initial temperature; ρ is the density; Φ_{abs} is the density of laser energy absorbed during the pulse; C_p is the specific heat capacity; d_T is the depth of thermal heating during the time $t = \tau$; and h is the gold layer thickness. Let us determine T in Eqn (1) for $\tau = 8$ ns, $E = 20$ μJ, $I = 0.4$ GW cm^{-2} (see Fig. 9), i.e., the case for which the absorption coefficient $K_f \approx 18\% \pm 4\%$ was found by the optoacoustic method. Then $\Phi_{abs} = K_f I\tau = 5.8$ kJ m^{-2} and, substituting the tabulated values ($\rho^g = 2500$ kg m^{-3}, $\rho^{gold} = 19\,320$ kg m^{-3}, $\rho^w = 1000$ kg m^{-3}, $C_p^g = 700$ J kg^{-1} K^{-1}, $C_p^{gold} = 128.7$ J kg^{-1} K^{-1}, $C_p^w = 4200$ J kg^{-1} K^{-1}) into Eqn (1) for $h = 50$ nm we obtain $T \approx 10^4$ K.

Since one of the factors affecting the cell systems in the process of the laser transfer can be the pulsed laser radiation passed through the absorbing film, we performed the experiments aimed at the study of the transmission coefficient T_{tr}. The spectrometric measurements (see Fig. 2) have shown that at small intensities of laser radiation the transmission coefficient of the gold film at the wavelength 1064 nm of the laser radiation amounts to ~0.15%. At such intensities, the major part of the laser energy is reflected from the film, and for the thickness 50 nm practically all the rest radiation is absorbed in the gold layer. The measurements performed in the range of laser pulse energies 5 μJ – 1 mJ at the pulse durations τ from 4 to 200 ns (Fig. 8) have shown that from 10% to 60% of energy passes through the substrate with the gold layer. The smallest transmission coefficient for the shortest ($\tau = 4$ ns) and the longest ($\tau = 200$ ns) laser pulses amounted to $6.1\% \pm 2.4\%$ (for $E = 24$ μJ) and $10.3\% \pm 2.5\%$ (for $E = 235$ μJ), respectively. At the fixed energy of laser radiation $E \geqslant 20$ μJ, one can observe a practically monotonic growth of the transmission coefficient T with increasing pulse duration τ (Fig. 8). Thus, the minimal doze of laser radiation that can affect the living cells transferred in the gel amounts to nearly 60 mJ cm^{-2}.

In our opinion, the observed high values of the coefficient transmission of the pulsed laser radiation by the donor plate with a gold film are explained by the following factors. By heating a metal to high temperatures (of order of the melting temperature and higher), the reflection coefficient sharply decreases [25] due to the metal–dielectric transition [28]. During the pulse, the gold film is partially destroyed. This explains an increase in the transmission coefficient with increasing E, observed for $\tau = 4$ ns and two first points for $\tau = 8$ and 20 ns (Fig. 8a). Further decrease in the transmission coefficient (Fig. 8b) is related to the growing absorption of radiation by the plasma [29] (Fig. 6).

Another factor affecting the cell systems in the process of laser microsampling can be the micro- and nanoparticles of gold transferred from the donor plate to the acceptor plate and appearing in the drop [30]. To study this issue, we performed the experiments on estimating the gold content in different forms in the gel droplets on the acceptor plate. It was found that at the acceptor plate inside the gel droplets and sometimes outside them one can find both microparticles (Fig. 10b) and nanoparticles of gold that can be distributed in the gel droplet chaotically (Fig. 10a) or even form structures (Fig. 10c). The amount of nanoparticles and their size distribution depend on the laser pulse energy and duration. We believe that the transfer of gold microparticles is caused by inhomogeneities of the gold film and its adhesion to the glass surface, and the nanoparticles are produced because of the fragmentation of the melted gold film, its explosive boiling and the process of self-assembly of gold atoms. The size distribution of nanoparticles both on the donor and on the acceptor plate (in the microdroplet) will depend on the film thickness, the energy, intensity and duration of the laser pulse, as well as the characteristics of the laser plasma [31]. At $\tau = 8$ ns (the pulses with $\tau = 10$ ns are applied in the microsampling of microorganisms [14]) the percentage of gold nanoparticles in the gel droplets exhibits virtually a linear dependence on E. If we relate the area occupied by the particles to the area of the hole in the gold film on the donor plate, then we can easily find the energy dependence (for 5 μJ $\leqslant E \leqslant$ 100 μJ) of the fraction (per cent) of gold that flew from the interaction area as $S_{Au\ hole} \approx E - 4$. Thus, the flight of nanoparticles begins at $E \approx 4$ μJ, and at $E = 100$ μJ the area occupied by nanoparticles on the acceptor plate almost coincides with the area of the hole in the gold film on the donor plate. If we assume that the size of nanoparticles is approximately equal to the gold layer thickness [which corresponds to the results of measurements based on SEM images (see Fig. 4)], then for $E = 100$ μJ all gold contained in the area of the hole in the gold film is deposited in the form of nanoparticles on the acceptor plate. Note that the filament patterns (Fig. 10c) can appear due to the oscillation of the jet carrying the gold nanoparticles [32].

The experiments on microsampling of gel with soil microparticles (carriers of microorganisms [14]) have shown that the addition of soil particles to the gel leads to considerable (by six times for $\tau = 8$ ns and $E = 20$ μJ) reduction of the jet velocity and increase in its transverse size (Fig. 11). Such changes are due to an increase in the gel viscosity after the addition of the soil particles. The size of soil particles in the microdroplet (Fig. 11) amounts to 1–30 μm, and there are sufficiently large individual particles among them that can serve as carriers of the colonies of microorganisms interesting for us.

The experiments carried out have shown that within the studied range of laser pulse durations and energies the minimal values of the transmission coefficient of the pulsed laser radiation with $\lambda = 1.064$ μm amounts to ~10%, i.e., in the process of microsampling, the living organisms receive a high doze of laser radiation. This dose can be reduced, e.g., by increasing the thickness of the metallic film. However, it should be taken into account that in this case the amount of gold micro- and nanoparticles transferred to the acceptor plate will also grow, which is undesirable since they can exert toxic influence on the microorganisms and cell systems [30].

5. Conclusions

In the present work, the thermal and transport processes that take place during the laser transfer (microprint) of gel microdroplets under the impact of the pulses of laser radiation with the wavelength 1.064 μm, the duration in the range 4–200 ns, and the energy from 2 μJ to 1 mJ are studied.

For the working regimes and $\tau = 8$ ns the maximal temperature in the laser impact area is estimated, which for $E = 20$ μJ amounts to $\sim 10^4$ K. It is shown that in the mechanism of laser-induced transfer an important role is played by the processes of explosive boiling in water (gel) and gold (the material of the absorbing coating of the donor plate).

It is found that within the entire studied range of the laser pulse parameters, the transmission coefficient of radiation with $\lambda = 1.064$ μm through the donor plate depends on the pulse duration and the density of its energy and varies within the range 10%–60%.

It is shown that there are two mechanisms of transferring gold to the acceptor plate related to: (i) the transfer of gold microparticles due to the inhomogeneities of the gold film and its adhesion and (ii) the transfer of gold atoms and nanoparticles produced by the explosive boiling of gold. It was found that at the laser pulse duration 8 ns and low energies ($E < 10$ μJ) the fraction of gold nanoparticles transferred to the acceptor plate is negligibly small; with the increase of the pulse energy it linearly grows.

It is found that when the particles of soil are added to the gel, the main influence on the process of jet formation is exerted by the increase in the substrate viscosity that leads to the reduction of jet velocity with a simultaneous increase in its transverse size. The performed studies allow optimisation of the processes of transferring gel microdroplets in rapidly developing technologies of laser bioprinting.

Acknowledgements. The work was supported by the RF Government's Grants Council (Support of Research Supervised by Leading Scientists Programme, Agreement No. 14.B25.31.0019).

References

1. Piqué A., Chrisey D.B., Auyeung R.C.Y., et al. *Appl. Phys. A*, **69** (1), 279 (1999).
2. Mathews S.A., Auyeung R.C.Y., Piqué A. *J. Laser Micro/Nanoeng.*, **2**, 103 (2007).
3. Narazaki A., Sato T., Kurosaki R., Kawaguchi Y., Niino H. *Appl. Phys. Express*, **5**, 057001 (2008).
4. Suzuki K. *Electr. Eng. Jpn.*, **165**, 60 (2008).
5. Unger C., Gruene M., Koch L., Koch J., Chichkov B.N. *Appl. Phys. A*, **103** (2), 271 (2011).
6. Kuznetsov A.I., Unger C., Koch J., Chichkov B.N. *Appl. Phys. A*, **106** (3), 479 (2012).
7. Ma H., Mismar W., Wang Y., Small D.W., Ras M., Allbritton N.L., Sims C.E., Venugopalan V. *J. R. Soc. Interface.*, **9**, 1156 (2011).
8. Chatzipetrou M., Tsekenis G., Tsouti V., Chatzandroulis S., Zergioti I. *Appl. Surf. Sci.*, **278**, 250 (2013).
9. Koch L., Kuhn S., Sorg H., et al. *Tissue Eng. Part C: Methods*, **16** (5), 847 (2009).
10. Nguyen A.K., Narayan R.J. *Ann. Biomed. Eng.*, **45** (1), 84 (2017).
11. Ovsianikov A., Gruene M., Pflaum M., Koch L., Maiorana F., Wilhelmi M., Haverich A., Chichkov B. *Biofabricat.*, **2** (1), 014104 (2010).
12. Serra P., Colina M., Fernández-Pradas J.M., Sevilla L., Morenza J.L. *Appl. Phys. Lett.*, **85** (9), 1639 (2004).
13. Deng Y., Renaud P., Guo Z., Huang Z., Chen Y. *J. Biol. Eng.*, **11** (1), 2 (2017).
14. Ringeisen B.R., Rincon K., Fitzgerald L.A., Fulmer P.A., Wu P.K. *Meth. Ecol. Evolut.*, **6** (2), 209 (2015).
15. Khmelnitsky R.A., Evlashin S.A., Martovitsky V.P., et al. *Cryst. Growth Des.*, **16** (3), 1420 (2016).
16. Zharov V.P., Letokhov V.S. *Laser Optoacoustic Spectroscopy* (Berlin: Springer, 1986).
17. Chudnovskii V.M., Yusupov V.I., Dydykin A.V., Nevozhay V.I., Kisilev A.Yu., Zhukov S.A., Bagratashvili V.N. *Quantum Electron.*, **47** (4), 361 (2017) [*Kvantovaya Elektron.*, **47** (4), 361 (2017)].
18. Kim D., Ye M., Grigoropoulos C.P. *Appl. Phys. A*, **67** (2), 169 (1998).
19. Park H.K., Kim D., Grigoropoulos C.P., Tam A.C. *J. Appl. Phys.*, **80** (7), 4072 (1996).
20. Hohlfeld J., Wellershoff S.S., Güdde J., Conrad U., Jähnke V., Matthias E. *Chem. Phys.*, **251** (1), 237 (2000).
21. Duocastella M., Fernández-Pradas J.M., Morenza J.L., Serra P. *J. Appl. Phys.*, **106** (8), 084907 (2009).
22. Mazhukin V.I., Samokhin A.A., Demin M.M., Shapranov A.V. *Quantum Electron.*, **44** (4), 283 (2014) [*Kvantovaya Elektron.*, **44** (4), 283 (2014)].
23. Yusupov V.I., Tsypina S.I., Bagratashvili V.N. *Laser Phys. Lett.*, **11** (11), 116001 (2014).
24. Kovalenko S.A., Fedorovych R.D. *Semicond. Phys. Quantum Electron. Optoelectron.*, **3** (3), 383 (2000).
25. Benavides O., de la Cruz May L., Mejia E.B., Hernandez J.R., Gil A.F. *Laser Phys.*, **26** (12), 126101 (2016).
26. Miotello A., Kelly R. *Appl. Phys. Lett.*, **67**, 3535 (1995).
27. Tsvetkov M.Yu., Minaev N.V., Akovantseva A.A., Pudovkina G.I., Timashev P.S., Tsypina S.I., Yusupov V.I., Muslimov A.E., Butashin A.V., Kanevsky V.M., Bagratashvili V.N. *Sverkhkriticheskiye Flyuidy: Teoriya i Praktika*, **12** (2), 68 (2017).
28. Bykovsky N.E., Pershin S.M., Samokhin A.A., Senatsky Yu.V. *Quantum Electron.*, **46** (2), 128 (2016) [*Kvantovaya Elektron.*, **46** (2), 128 (2016)].
29. Bulgakov A.V., Bulgakova N.M. *Quantum Electron.*, **29** (5), 433 (1999) [*Kvantovaya Elektronika*, **27** (2), 154 (1999)].
30. Shamaila S., Zafar N., Riaz S., Sharif R., Nazir J., Naseem S. *Nanomater.*, **6** (4), 71 (2016).
31. Serkov A.A., Kuz'min P.G., Rakov I.I., Shafeev G.A. *Quantum Electron.*, **46** (8), 713 (2016) [*Kvantovaya Elektron.*, **46** (8), 713 (2016)].
32. Brown M.S., Kattamis N.T., Arnold C.B. *Microfluid. Nanofluid.*, **11** (2), 199 (2011).